Optimizing image reconstruction for simultaneous sub-mm clustered pinhole PET-SPECT

Marlies C. Goorden, Frans van der Have, and Freek J. Beekman

***Abstract*— A newly developed Versatile Emission Computed Tomography system (VECTor) enables simultaneous imaging of SPECT and PET tracer molecule distributions at sub-mm resolutions in mice. VECTor uses a dedicated collimator with clusters of small opening-angle pinholes that is mounted on a SPECT system with stationary NaI detectors. The novel pinhole geometry and the extended energy range of imaged gamma photons require a new evaluation of image reconstruction software instead of only slightly adapting standard SPECT methods. The preliminary results presented in this paper demonstrate that such a reconstruction optimization strongly improves VECTor's performance.**

Projections from different pinholes slightly overlap on the 3 gamma detectors of VECTor. Near the edges of the pinhole projections, a small amount of mismodeling -which is often unavoidable- leads to a large loss of information about the emission direction of the detected gamma photons. We tested if uniformity of SPECT images was improved by simply ignoring detector pixels located near the pinhole projection edges. Secondly, we investigated if accurately modeling the varying depth-of-interaction (DOI) in the NaI detector and including a larger portion of the point spread function (PSF) tails improved PET resolution phantom images.

Reconstructed SPECT images of a syringe were most uniform when the detector pixels within a 1 to 2 pixel distance from the edges of the pinhole projections were ignored. Furthermore, we found a remarkable improvement in PET resolution phantom reconstructions when a large portion of the PSF tails was used in the reconstruction and when DOI was modeled. To conclude, we have shown that the performance of VECTor can be significantly improved by optimizing its image reconstruction software.

***Index Terms*—SPECT, PET, pinholes, fully 3D iterative reconstruction**

I. Introduction

SPECT and PET imaging of small animals has recently been combined in a single Versatile Emission Computed Tomography system (VECTor) [1]. VECTor attains cutting edge image resolution (<0.5 mm) for SPECT while simultaneously imaging PET tracers at sub-mm resolutions. An example of quadruple PET-SPECT tracer imaging in a mouse is displayed in Fig. 1. Since VECTor fully integrates PET and SPECT, the tracer distributions in such an image are perfectly aligned in space and time and can therefore be directly correlated. As a consequence, VECTor enables a whole new range of applications in biomedical research, notably applications in which the correlation of multiple biological processes is of importance.

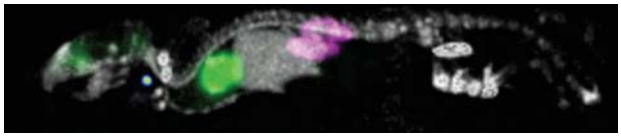

Fig. 1. Simultaneous PET-SPECT quadruple isotope imaging with VECTor. Maximum Intensity Projection are shown of a 60 minute total body mouse scan with 100 MBq ^{99m}Tc-HDP (Gray), 35 MBq ^{18}F-FDG (Green), 19 MBq ^{111}In-Pentetreotide (Magenta), and 5 MBq ^{123}I-NaI (Rainbow).

VECTor is based on a novel collimation technique that exploits clusters of pinholes [2, 3] with each cluster sampling the same field-of-view as a single traditional pinhole (Fig. 2(a)). Since each of the pinholes in the cluster has a relatively small opening angle, pinhole edge penetration –which would be a major problem when imaging 511 keV annihilation photons with a standard SPECT collimator- is reduced. The clustered pinhole collimator is placed into a SPECT system with stationary NaI gamma detectors (U-SPECT-II, MILabs BV, The Netherlands [4]).

A key ingredient to obtaining high-resolution images with complex pinhole geometries is the use of iterative reconstruction algorithms that (partly) compensate for effects like spatially variant sensitivity and resolution. Ideally, these algorithms are based on an accurate knowledge of point spread functions (PSFs), the system's response to a point source. For practical reasons, we require that VECTor is calibrated with a limited number of point source measurement of a single isotope (^{99m}Tc) but we model the energy dependent PSFs for each isotope individually.

Being a new modality, optimizing VECTor's image reconstruction software may have a significant impact on its performance. This is confirmed by the preliminary results that we present in this paper. We have focused on aspects in which VECTor differs from the standard U-SPECT-II collimators. First, in contrast to these standard collimators, the projections of the clustered pinholes onto the 3 gamma

M. C. Goorden is with Delft University of Technology, Section Radiation Detection and Matter, Mekelweg 15, 2629 JB Delft, The Netherlands (e-mail: m.c.goorden@tudelft.nl).

F. van der Have and F.J. Beekman are with Delft University of Technology, Section Radiation Detection and Matter, Mekelweg 15, 2629 JB Delft, The Netherlands and MILabs, Utrecht, The Netherlands.

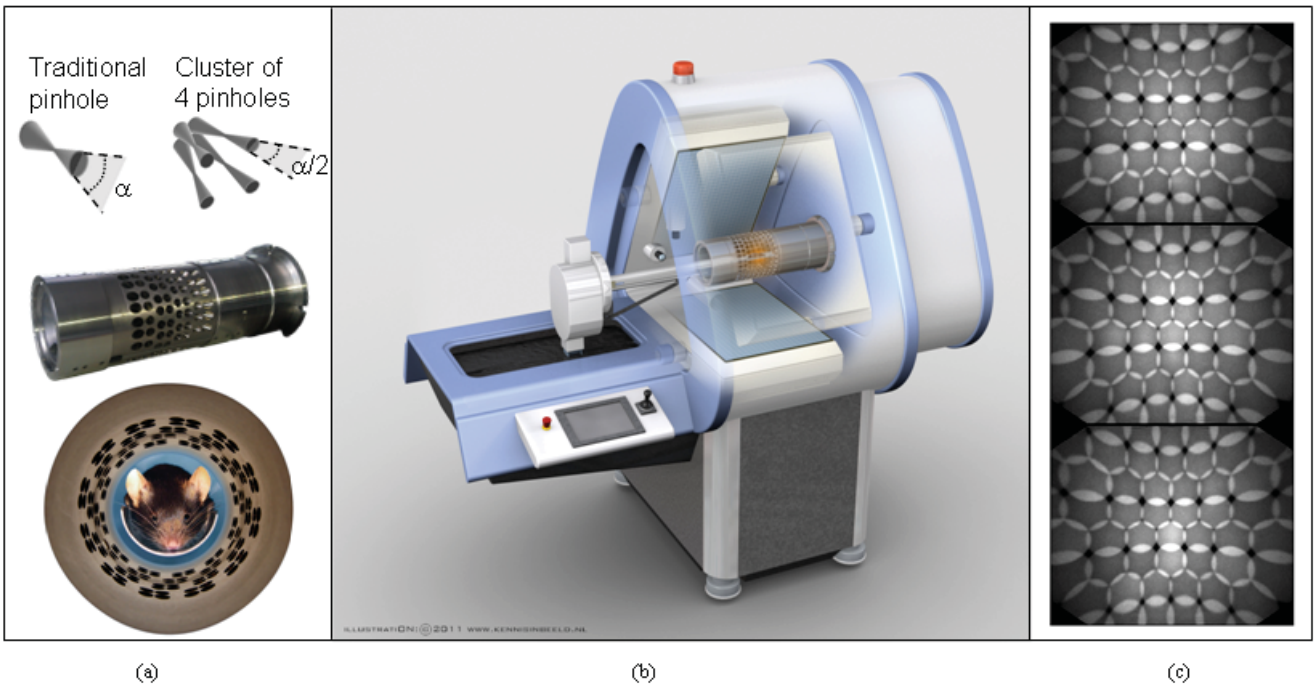

Fig. 2. Integration of the clustered multi-pinhole collimator into an existing SPECT/CT platform. (a) A traditional pinhole with opening angle α and a cluster of four pinholes with approximately the same field-of-view and opening angle α/2. The clustered multi-pinhole collimator optimized for imaging SPECT and PET tracers, into which a mouse is placed, contains 48 cluster of 4 pinholes each. (b) The collimator is mounted in a SPECT/CT system with three large-area gamma detectors. (c) Projection image of an extended ^{99m}Tc source onto the detector; pinhole projections slightly overlap. Subfigures (a) and (b) were reprinted from [1].

detectors of the system slightly overlap when an extended source is imaged (Fig. 2(c)). Note that across the edge of the ellipsoidal projection area belonging to a certain pinhole, a very abrupt change occurs in the probability that a detected gamma photon originated from that pinhole. This means that even a slight amount of mismodeling of the exact location of these edges, which can occur due to manufacturing uncertainties, leads to a considerable loss of information about the emission direction of gamma photons detected near these edges. Therefore, for some detector pixels in these edge regions, the sensitivity that is gained when their signal is used in the image forming process may be completely offset by the ambiguous information they carry. With this in mind, we investigated if it helped to simply ignore the signal of certain detector pixels in image reconstruction. Secondly, high-energy annihilation gammas have broad PSFs with longer tails than is common in SPECT as well as an increased variation of the depth-of-interaction (DOI) in the gamma detector. We investigated whether including the tails and the varying DOI into the PSF model visually improved PET images.

II. METHODS

A. Pinhole Geometry and System description

The clustered pinhole collimator (Fig. 2(a)) contains 48 clusters of four pinholes placed in four rings. It was integrated into the U-SPECT-II/CT system [4] which has three large-area NaI(Tl) gamma detectors placed in a triangular set-up (Fig. 2(b)). The projection of an extended ^{99m}Tc source on the 3 gamma detectors is shown in Fig. 2(c); projections of different pinholes slightly overlap. A detailed description of the collimator geometry can be found in [1].

B. Image reconstruction and calibration

The scanning focus method [5] was used for data acquisition. A Pixel-based Ordered Subsets Expectation Maximization (POSEM) algorithm with 32 subsets was used for image reconstruction [6]. Scatter was corrected for by using a standard triple energy window correction [7].

A ^{99m}Tc point source measurement [8] was done to correct for small geometrical misalignments that can occur due to slight rotations and translations of the collimator or the gamma detectors with respect to the expected (designed) position and orientation. The detector position model used in the fit was based on projecting a point source location through the pinhole centers on the detector plane [8]. Since an arbitrary translation + rotation can be described by 6 parameters, we fitted 24 system parameters to the point source experiment (3 detectors + 1 collimator). It was assumed that relative pinhole positions and orientations in the collimator were as designed.

Based on this fit, PSFs were calculated with a ray tracing code that calculated the path length L of gamma photons through the collimator material. In our code, we could set a cut-off C which had the effect to only save those parts of the PSFs with attenuation $\exp(-\mu L)>C$. Here μ is the collimator's energy dependent attenuation coefficient. Furthermore, the varying DOI in the gamma detector was modeled by also using a ray tracing code for the NaI scintillator. In our code, DOI modeling could be turned on/

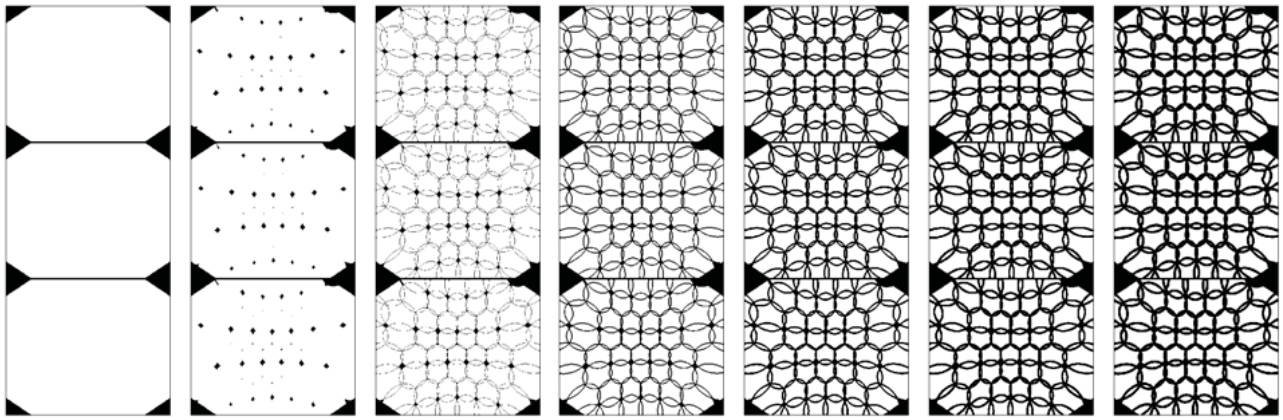

(a) (b) (c) (d) (e) (f) (g)

Fig. 3. Different detector masks that were applied in system matrix generation; the black areas represent those pixels that were *not* used in image reconstruction. (a) The active area of the 3 gamma detectors was fully used. (b) Pixels not contained in any pinhole projection were ignored. (c) Pixels at the edges of the pinhole projections were also left out. In subsequent masks, pixels within a 1, 2, 3 and 4 pixel distance were also ignored (d-g).

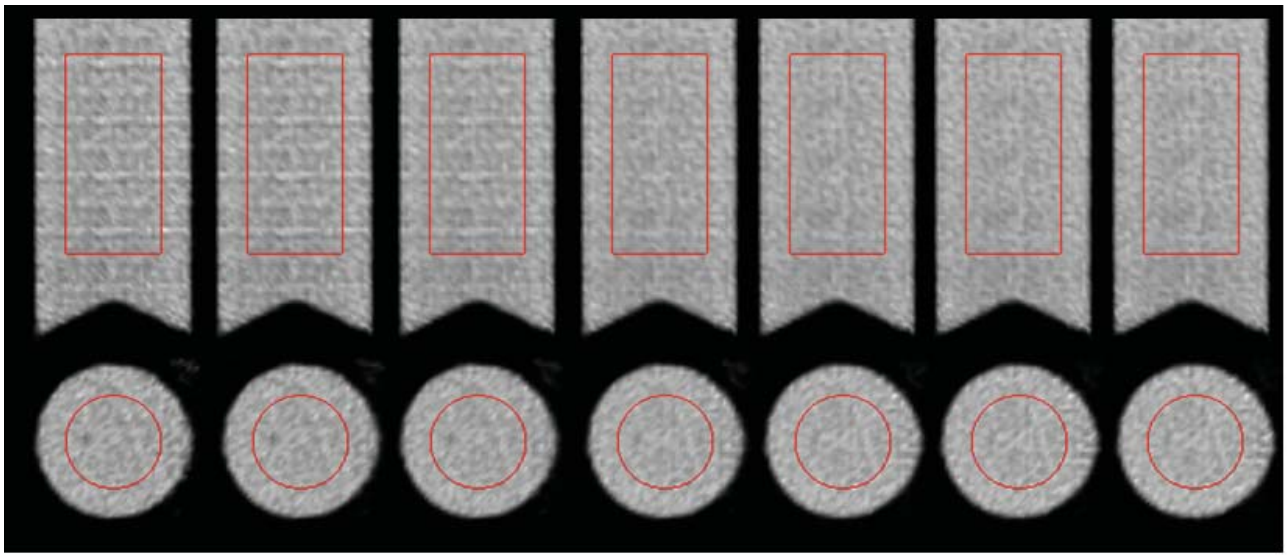

Uniformity: 17.5% (a) 15.4% (b) 13.7% (c) 12.9% (d) 13.0% (e) 13.2% (f) 13.5% (g)

Fig. 4. Two mutually perpendicular slices (slice thickness 2mm) through reconstructions of a 12 ml syringe filled with ^{99m}Tc. Reconstructions (a)-(g) correspond to detector masks of Fig. 3 with the same label. Uniformity in the cylindrical region-of-interest (red line) is provided below each reconstruction as a percentage of the mean activity in the same region.

off at will. When DOI modeling was used in the ray tracing code, a DOI correction was also used in the detector position model for the point source fit. Detector resolution was modeled by a Gaussian detector response with 3.5 mm FWHM. Finally, our code read in a detector mask in which some of the detector pixels could be set to zero and therefore not be incorporated in the system matrix.

C. Reconstruction optimization

The pinhole projection areas for each pinhole were determined by means of fitting overlapping ellipses to the measured ^{99m}Tc flood source projection (Fig. 2(c)), where the position of the center, length of major and minor axes and angle of each of the ellipses were fit parameters. We tested different detector masks (Fig. 3). The basis was formed by mask (a) which included all active detector pixels. We subsequently left out more and more pixels; first those that were not located in at least 1 of the ellipsoidal pinhole projections (b), subsequently pixels at the edges of the pinhole projections (c) and then all pixels within a 1, 2, 3 or 4 pixel distance from the edges (d-g). Compared to Fig. 3(a), masks (b-g) contained 97%, 92%, 82%, 73%, 67%, 62% of the pixels, respectively. We tested how use of these masks influenced uniformity in reconstructions of a 12 ml syringe filled with 225 MBq ^{99m}Tc and scanned for 9 hours. These tests were done for a cut-off C=20% and no DOI modeling.

Secondly, we lowered C from 20% to 1% and subsequently incorporated DOI modeling. For this, we assumed an attenuation coefficient of 0.012 mm^{-1} in the NaI scintillator based on previous simulations and experiments [9]. We tested how changing these parameters influenced PET resolution phantom images. To this purpose, a Jaszczak resolution phantom with capillary diameters of 0.7-1.5 mm was filled with 102 MBq ^{18}F solution and

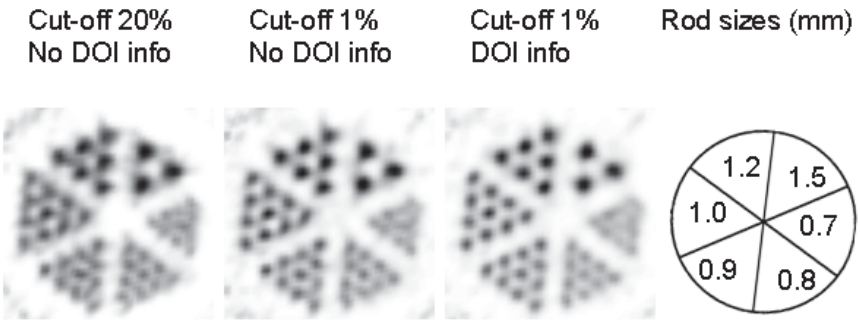

Fig. 5. PET images of a resolution phantom. (a) System matrix generated with a cut-off of 20% and no DOI modeling. (b) System matrix generated with a lower cut-off of 1%, DOI modeling not included. (c). Cut-off kept at 1%, DOI modeling included. (d) Rod sizes in each segment. Slice thickness of the reconstructions was 2 mm.

scanned for 4 hours. The distance between capillary centers was equal to twice the capillary diameter.

RESULTS

In Fig. 4 we show slices through the ^{99m}Tc uniform phantom reconstructions for all tested detector masks. Below each of the reconstructions, uniformity in a cylindrical region-of-interest (also shown) is provided as a percentage of the mean activity in the same region. Clearly, line-shaped artifacts are present in Fig. 4(a) which uses all detector pixels in the active detector area. As one does not use detector pixels in areas outside the pinhole projections (Fig. 4(b)) and leaves out more and more pixels near the edges (Fig. 4(c)-4(g)), these artifacts gradually disappear. Both visual inspection and calculated uniformity indicate that there is an optimum; it is best to leave out all pixels within a 1 or 2 pixel distance from the edges (Fig. 4(d) and 4(e)).

PET images of the resolution phantom are shown in Fig. 5. Lowering the cut-off from 20% (a) to 1% (b) resulted in images which appear less noisy. However, the rods in 5(a) and 5(b) are somewhat triangularly shaped. Including DOI modeling into the matrix generation obliterates this effect (c). In the latter figure there is no visual deformation of rods.

III. DISCUSSION AND CONCLUSION

In this paper, we have very convincingly demonstrated that optimizing image reconstruction software of VECTor can significantly improve image quality. We found that uniformity in SPECT images improves if one ignores the gamma photons detected in detector pixels near the edges of the pinhole projections. Images with the best uniformity only used 70 to 80% of the detector pixels. Apparently, the increased sensitivity that is obtained if these gamma photons would be taken into account does not outweigh the ambiguous information they carry. This is reminiscent of what other studies have found on the effect of overlapping pinhole projections on reconstructions [10, 11].

Furthermore, we found that for imaging high-energy annihilation photons resulting from PET tracers, it is important to model large portions of the PSF tails and to also model the variable DOI in the gamma detector. Such modeling has a significant impact on the appearance and visibility of small structures.

Here we have presented preliminary results. In the near future we plan to extend our study to systematically investigate the influence and interplay of these parameters on SPECT, PET and combined SPECT-PET images of several phantom and animal scans.

REFERENCES

[1] M. C. Goorden, F. van der Have, R. Kreuger, R. M. Ramakers, B. Vastenhouw, J. P. H. Burbach, J. Booij, C. F. M. Molthoff, and F. J. Beekman, "VECTor: A Preclinical Imaging System for Simultaneous Submillimeter SPECT and PET," Journal of Nuclear Medicine, vol. 54, no. 2, pp. 306-312, 2013.

[2] F. J. Beekman, "A focused pinhole gamma detection device," EP20730392009

[3] M. C. Goorden and F. J. Beekman, "High-resolution tomography of positron emitters with clustered pinhole SPECT," Physics in Medicine and Biology, vol. 55, no. 5, pp. 1265-1277, 2010.

[4] F. van der Have, B. Vastenhouw, R. M. Ramakers, W. Branderhorst, J. O. Krah, C. Ji, S. G. Staelens, and F. J. Beekman, "U-SPECT-II: an ultra-high-resolution device for molecular small-animal imaging," Journal of Nuclear Medicine, vol. 50, no. 4, pp. 599-605, 2009.

[5] B. Vastenhouw and F. J. Beekman, "Submillimeter total-body murine imaging with U-SPECT-I," Journal of Nuclear Medicine, vol. 48, no. 3, pp. 487-493, 2007.

[6] W. Branderhorst, B. Vastenhouw, and F. J. Beekman, "Pixel-based subsets for rapid multi-pinhole SPECT reconstruction," Physics in Medicine and Biology, vol. 55, no. 7, pp. 2023-2034, 2010.

[7] K. Ogawa, Y. Harata, T. Ichihara, A. Kubo, and S. Hashimoto, "A practical method for position-dependent Compton-scatter correction in single photon-emission ct," IEEE Transactions on Medical Imaging, vol. 10, no. 3, pp. 408-412, 1991.

[8] F. van der Have, B. Vastenhouw, M. Rentmeester, and F. J. Beekman "System calibration and statistical image reconstruction for ultra-high resolution stationary pinhole SPECT," IEEE Transactions on Medical Imaging, vol. 27, no. 7, pp. 960-971, 2008.

[9] M. C. Goorden, F. van der Have, R. Kreuger, and F. J. Beekman, "An efficient simulator for pinhole imaging of PET isotopes," Physics in Medicine and Biology, vol. 56, no. 6, pp. 1617-1634, 2011.

[10] K. Vunckx, P. Suetens, and J. Nuyts, "Effect of overlapping projections on reconstruction image quality in multipinhole SPECT," IEEE Transaction on Medical Imaging, vol. 27, no. 7, pp. 972-983, 2008.

[11] G. S. Mok, B. M. Tsui, and F. J. Beekman, "The effects of object activity distribution on multiplexing multi-pinhole SPECT," Physics in Medicine and Biology, vol. 56, no. 8 pp. 2635-2650, 2011.